



Acoustic attenuation due to transformation twins in CaCl_2 : Analogue behaviour for stishovite

Zhiying Zhang^{a,*}, Wilfried Schranz^b, Michael A. Carpenter^a

^a Department of Earth Sciences, University of Cambridge, Downing Street, Cambridge CB2 3EQ, United Kingdom

^b Faculty of Physics, University of Vienna, Strudlhofgasse 4, A-1090 Vienna, Austria

ARTICLE INFO

Article history:

Received 18 April 2012

Received in revised form 4 July 2012

Accepted 9 July 2012

Available online 20 July 2012

Edited by Kei Hirose

Keywords:

Pseudoproper ferroelastic phase transition

Ferroelastic twin walls

Stishovite

CaCl_2

Acoustic attenuation

ABSTRACT

CaCl_2 undergoes a tetragonal ($P4_2/mnm$) to orthorhombic ($Pnmm$) transition as a function of temperature which is essentially the same as occurs in stishovite at high pressures. It can therefore be used as a convenient analogue material for experimental studies. In order to investigate variations in elastic properties associated with the transition and possible anelastic loss behaviour related to the mobility of ferroelastic twin walls in the orthorhombic phase, the transition in polycrystalline CaCl_2 has been examined using resonant ultrasound spectroscopy (RUS) at high frequencies (0.1–1.5 MHz) in the temperature interval 7–626 K, and dynamic mechanical analysis (DMA) at low frequencies (0.1–50 Hz) in the temperature interval 378–771 K. RUS data show steep softening of the shear modulus as the transition temperature is approached from above and substantial acoustic dissipation in the stability field of the orthorhombic structure. DMA data show softening of the storage modulus, which continues through to a minimum ~ 20 K below the transition point and is followed by stiffening with further lowering of temperature. There is no obvious acoustic dissipation associated with the transition, as measured by $\tan \delta$, however. The elastic softening and stiffening matches the pattern expected for a pseudoproper ferroelastic transition as predicted elsewhere. Acoustic loss behaviour at high frequencies fits with the pattern of behaviour expected for a twin wall loss mechanism but with relaxation times in the vicinity of $\sim 10^{-6}$ s. With such short relaxation times, the shear modulus of CaCl_2 at frequencies corresponding to seismic frequencies would include relaxations of the twin walls and is therefore likely to be significantly lower than the intrinsic shear modulus. If these characteristics apply also to twin wall mobility in stishovite, the seismic signature of the orthorhombic phase should be an unusually soft shear modulus but with no increase in attenuation.

© 2012 Elsevier B.V. All rights reserved.

1. Introduction

The high pressure phase transition in stishovite (SiO_2), between tetragonal ($P4_2/mnm$) and orthorhombic ($Pnmm$) structures, has attracted a great deal of recent attention both from its intrinsic interest in terms of physical properties related to pseudoproper ferroelastic behaviour (Tsuchida and Yagi, 1989; Matsui and Tsuneyuki, 1992; Cohen, 1992, 1994; Lacks and Gordon, 1993; Mao et al., 1994; Kingma et al., 1995, 1996; Lee and Gonze, 1995, 1997; Dubrovinsky and Belonoshko, 1996; Karki et al., 1997a,b; Andraut et al., 1998, 2003; Carpenter et al., 2000; Ono et al., 2002a; Carpenter, 2006; Hemley et al., 1994, 2000a,b; Akins and Ahrens, 2002; Shieh et al., 2002, 2005; Cordier et al., 2004; Tsuchiya et al., 2004; Lakshtanov et al., 2007b; Togo et al., 2008; Jiang et al., 2009; Bolfan-Casanova et al., 2009; Driver et al., 2010) and because these might have a direct influence on the seismic properties of

subducted oceanic slabs (e.g. Kaneshima and Helffrich, 2010; Vinik et al., 2010; Nomura et al., 2010). From a geophysical perspective, the properties of interest are primarily elastic, and it is clear that the phase transition will give rise to marked softening of the shear modulus as the transition point is approached from the stability fields of both the tetragonal and orthorhombic structures as a consequence of softening of the single crystal elastic constants (C_{11} – C_{12}) (Cohen, 1992, 1994; Matsui and Tsuneyuki, 1992; Lacks and Gordon, 1993; Lee and Gonze, 1995; Dubrovinsky and Belonoshko, 1996; Karki et al., 1997a,b; Hemley et al., 2000b; Carpenter et al., 2000; Shieh et al., 2002; Andraut et al., 2003; Carpenter, 2006; Lakshtanov et al., 2007b; Togo et al., 2008; Jiang et al., 2009; Bolfan-Casanova et al., 2009; Driver et al., 2010). If the relevant mantle geotherm crosses the transition in pressure and temperature space, it follows that the geophysical signal indicative of the presence of stishovite will be a characteristic pattern of velocity changes for both P and S waves. As in the case of the $\beta \leftrightarrow \alpha$ transition in quartz (e.g. Carpenter et al., 1998; Mechie et al., 2004; Carpenter, 2006), knowledge of the phase boundary could then help to

* Corresponding author.

E-mail address: zhiyingzhang06@hotmail.co.uk (Z. Zhang).

constrain the local geotherm. A much smaller anomaly is expected in the bulk modulus (e.g. Carpenter et al., 2000; Andrault et al., 2003; Carpenter, 2006; Bolfan-Casanova et al., 2009), but this would be a more subtle effect and is altogether harder to detect even under laboratory conditions.

Another characteristic feature of ferroelastic phase transitions which is certainly relevant in the geophysical context is acoustic attenuation. This may be intrinsic (i.e. related to a pervasive influence such as critical slowing down) in the vicinity of the transition point or extrinsic (i.e. related to defects) over a much wider interval of temperature and pressure due to the mobility under stress of twin walls in the low symmetry phase (e.g. Carpenter and Zhang, 2011). Interest in anelastic effects more generally has been stimulated by the recognition that their temperature dependence is quite different from that of the elastic constants and, hence, that they could in principle provide a means of discriminating between the effects of temperature and composition (e.g. Romanowicz, 1995; Karato and Karki, 2001; Gung and Romanowicz, 2004; Brodholt et al., 2007; Matas and Bukowinski, 2007; Lekic et al., 2009; Carpenter and Zhang, 2011). The expectation is that, for most of the earth, seismic attenuation will be dominated by the anelastic properties of grain boundaries (e.g. Tan et al., 2001; Jackson et al., 2002; Webb and Jackson, 2003; Faul and Jackson, 2005; Jackson, 2007; Salje, 2008) and dislocations (e.g. Gueguen et al., 1989; Farla et al., 2012). However, recent investigations of the dynamics of twin walls in perovskites have shown that loss mechanisms associated specifically with the mobility under dynamic stress of twin walls could be really quite substantial (e.g. Harrison and Redfern, 2002; Harrison et al., 2004b,c; Carpenter, 2006; Carpenter et al., 2010; Daraktchiev et al., 2006, 2007; Walsh et al., 2008; McKnight et al., 2009a,b; Zhang et al., 2010a,b; Carpenter and Zhang, 2011).

Such considerations immediately raise the question, as discussed by Carpenter et al. (2000), of whether there could also be significant attenuation of seismic waves due to the presence of transformation twins in orthorhombic stishovite and, if so, what temperature-, pressure- and frequency-dependence it might show. Unfortunately, these are not easy questions to address directly for stishovite itself due to the inherent difficulty in trying to measure anelastic properties at high pressures. An alternative and more tractable approach is to start with an analogue material which should show the same behaviour in principle but under more easily accessible laboratory conditions. The primary objective of the present study was to show unambiguously that twin-wall related loss mechanisms could occur in CaCl_2 , which undergoes the same phase transition as occurs in stishovite but as a function of temperature at ambient pressure rather than as a function of pressure. Data are presented from resonant ultrasound spectroscopy (RUS) and dynamic mechanical analysis (DMA) at high frequencies (0.1–1.5 MHz) in the temperature interval ~ 7 –626 K, and at low frequencies (0.1–50 Hz) in the temperature interval ~ 378 –771 K, respectively.

As in stishovite, the $P4_2/mmm \leftrightarrow Pnm$ transition in CaCl_2 is driven by a soft optic mode which induces softening of an acoustic mode by bilinear coupling of the order parameter with the symmetry-breaking strain (Unruh et al., 1992; Unruh, 1993; Valgoma et al., 2002). From measurements of the lattice parameters and, hence, determinations of the spontaneous strain, it is known also that the transition is second order in both cases and is expected to conform closely to the precepts of Landau theory (Unruh, 1993; Carpenter et al., 2000; Howard et al., 2005). The transition temperature is ~ 491 K (Table 1; Bärnighausen et al., 1984; Anselment, 1985; Unruh et al., 1992; Unruh, 1993; Howard et al., 2005). The same transition is also observed as a function of temperature in CaBr_2 (Raptis et al., 1989; Raptis and McGreevy, 1991; Hahn and Unruh, 1991; Unruh, 1993; Kennedy and Howard, 2004; Howard et al., 2005), and ferroelastic twins have been observed in this

Table 1Summary of transition temperature for CaCl_2 detected using different methods.

Method	Sample	Transition temperature (K)	Reference
XRD	Powder	491	Bärnighausen et al. (1984)
XRD	Powder	491	Anselment (1985)
Raman spectroscopy	Pellet	491	Unruh et al. (1992) and Unruh (1993)
Synchrotron XRD	Powder	508	Howard et al. (2005)

material by optical microscopy at room temperature (Unruh, 1993). It is observed as a function of pressure in a much wider range of materials, including MgF_2 (Haines et al., 2001; Kanchana et al., 2003; Zhang et al., 2008; Kusaba and Kikegawa, 2008b), FeF_2 (Wang et al., 2011), CoF_2 (Wang et al., 2011), NiF_2 (Wang et al., 2011), ZnF_2 (Perakis et al., 2005; Kusaba and Kilegawa, 2008a), TiO_2 (Nagel and O'Keefe, 1971; Fritz, 1974), MnO_2 (Haines et al., 1995), GeO_2 (Haines et al., 1998, 2000; Lodziana et al., 2001; Ono et al., 2002b), RuO_2 (Haines and Leger, 1993; Ono and Mibe, 2011), SnO_2 (Haines and Leger, 1997; Haines et al., 1997; Parlinski and Kawazoe, 2000; Hellwig et al., 2003), PbO_2 (Haines et al., 1996), and MgH_2 (Zhang et al., 2007).

2. Experimental methods

Anhydrous CaCl_2 powder purchased from Sigma–Aldrich was ground using a mortar and pestle inside a glove box flushed with nitrogen gas. Pellets with diameter 13 mm were prepared by pressing the ground up powder under a pressure of ~ 60 bars for 1 min. These were then fired in air as follows: (1) heat from 373 to 673 K at 5 K/min; (2) hold at 673 K for 2 h; (3) heat from 673 to 773 K at 3 K/min; (4) hold at 773 K for 48 h; (5) cool from 773 to 383 K at 3 K/min. Rectangular parallelepiped samples were cut from the pellets using an annular diamond saw lubricated with paraffin. For RUS measurements, the parallelepiped of CaCl_2 had dimensions $4.260 \times 3.143 \times 3.039$ mm³, mass 0.0577 g. The density calculated from these dimensions is 1.418 g/cm³, which is 64% of the theoretical density, 2.20 g/cm³, based on lattice parameters at 300 K given by Unruh (1993). For DMA tests, the sample had dimensions $1.268 \times 1.743 \times 3.713$ mm³. Anhydrous CaCl_2 is very sensitive to moisture, and the samples were therefore kept in a desiccator with P_2O_5 powder as desiccant.

An offcut from the pellets used to make the RUS and DMA samples was crushed, immersed in a refractive index oil and examined in a polarising optical microscope. Birefringent grains up to ~ 5 –10 μm wide could be seen and some of these contained planar or lamellar features, indicating the presence of transformation twins arising from the tetragonal \rightarrow orthorhombic transition during cooling from the annealing temperature.

High temperature RUS data were collected in the frequency range 0.1–1.5 MHz with a step size of 28 Hz (50,000 data points per spectrum) using alumina buffer rods protruding into a horizontal Netzsch furnace (McKnight et al., 2008) and Stanford electronics described by Migliori and Maynard (2005). The sample was tested during repeated heating and cooling within the temperature range 386–626 K, with temperature steps of 2 K. During the last run, temperature was lowered to 291 K. The signal was generally weak but these repeated measurements revealed an overall pattern of peak variations which appeared to be systematic and could be analysed further. Low temperature RUS data were collected with the same frequency range and step size of 5 K between 7 and 307 K during cooling and heating using dynamic resonance system (DRS) Modulus II electronics and an Orange helium flow cryostat, as described by McKnight et al. (2007). Spectra collected from the low temperature instrument are always stronger than those obtained from the

high temperature instrument, because the sample sits directly on the transducers in the former, but is separated from the transducers by the length of the alumina rods in the latter.

DMA measurements were undertaken by parallel plate compression using a Diamond DMA from PerkinElmer over the temperature range 378–771 K, with a heating and cooling rate of 3 K/min. Static (F_s) and dynamic forces (F_d) were applied in the frequency range 0.1–50 Hz using a steel rod. There is a phase lag, δ , between the applied force and the response of the sample, which is measured as the displacement of the rod, u_d . Energy dissipation is given by

$$\tan \delta = E''/E', \quad (1)$$

where E'' is the loss modulus (i.e. the imaginary component of complex Young's modulus E) and E' is the storage modulus (i.e. real component of E) and the Young's modulus is given by

$$E = hF_d \exp(i\delta)/(Au_d), \quad (2)$$

where h is the height of the sample, 3.713 mm, and A is the base area of the sample, 2.210 mm².

3. Results

Fig. 1 shows segments of RUS spectra in the form of stacks with offsets up the y-axis in proportion to the temperatures at which they were collected. Regularly spaced background peaks at high temperatures which do not change frequency to any great extent with temperature are seen in all spectra collected with the high temperature instrument (e.g. Thomson et al., 2010; Zhang et al., 2011) and are due to the alumina buffer rods. At least some of the noisy background at very low temperatures arises from somewhere in the sample holder rather than from the sample itself. All the resonance peaks shift to lower frequency (elastic softening) with decreasing temperature and disappear below 481 K. They are not detectable in spectra collected in the high temperature instrument between 481 K and room temperature. Low amplitude peaks are easily visible in spectra from the low temperature instrument, however, due to the advantage of having the sample located directly on the transducers rather than at the end of alumina rods, remote from the transducers. With further decrease in temperature, the peaks shift to higher frequencies (elastic stiffening). At the lowest temperatures, weak peaks appear to be present but their trajectory is hard to follow due to noise.

Most resonance modes of a parallelepiped are dominated by shearing modes and, hence, their frequencies are dominated by combinations of shear elastic constants. For a polycrystalline sample this means that most modes provide direct information relating to the temperature dependence of the shear modulus. If the sample is isotropic, values of the shear and bulk moduli can be obtained by simultaneous fitting to a number of resonance frequencies. If, as in the present case, there is some anisotropy, it is not possible to obtain fits so easily.

In the present study the primary objective was to follow the temperature dependence of a shear modulus that contains contributions from (C_{11} – C_{12}) through the ferroelastic phase transition, and to determine whether there is significant attenuation within the stability field of the orthorhombic phase. These properties can be followed from measurements of a single resonance which depends on the shear modulus, G . Normal experience of RUS measurements on polycrystalline parallelepipeds is that the modes with lowest frequencies are dependent almost exclusively on G and the lowest frequency mode has therefore been used for evaluation. In this case the normalised square of frequency (f/f_0)² is proportional to the shear modulus, as

$$(f/f_0)^2 = G/G_0, \quad (3)$$

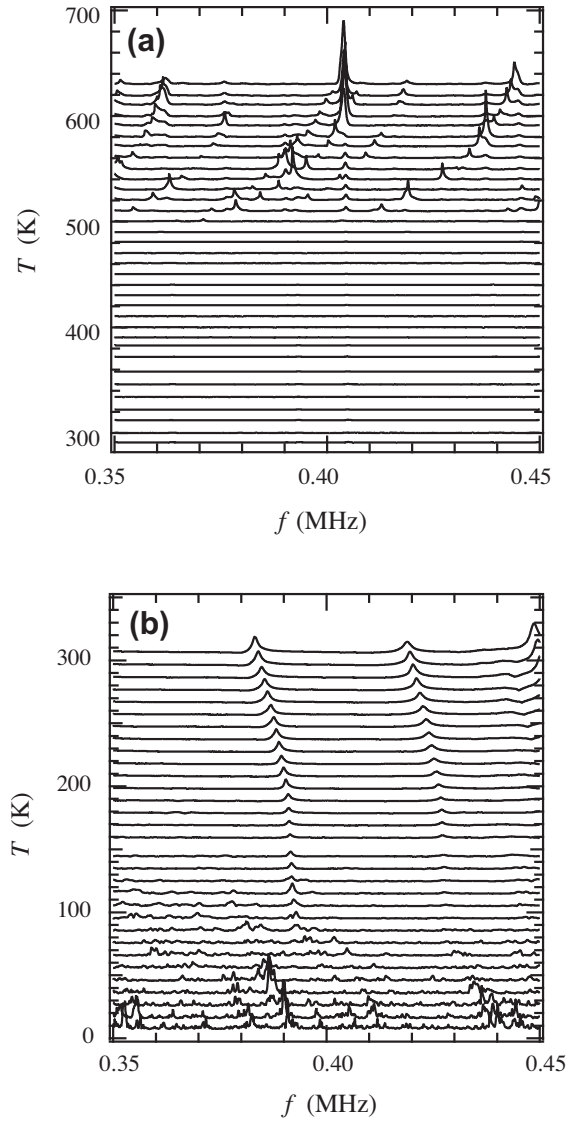


Fig. 1. Stacks of RUS scans for CaCl₂. (a) High temperatures. Regularly spaced background peaks are due to the alumina buffer rods. (b) Low temperatures. The background peaks at very low temperatures are noise from somewhere in the sample holder.

where f_0 and G_0 are the resonance frequency and shear modulus at some reference temperature. As a simple matter of convenience, the reference temperature was chosen to be 626 K.

Values of the inverse quality factor, Q^{-1} , were obtained from fitting an asymmetric Lorentzian function to individual resonance peaks as

$$Q^{-1} = \Delta f/f, \quad (4)$$

where f is the frequency of the peak and Δf its full width at half maximum amplitude. Strictly speaking, absolute values of Q^{-1} for comparison with other measures of damping should be obtained from fitting to the square of the amplitude, but the difference is only a factor of $\sim\sqrt{3}$ (see, for example, Lee et al., 2000; Lakes, 2004). The resulting temperature dependencies of $(f/f_0)^2$ and Q^{-1} are shown in Fig. 2. Note that no f^2 and Q^{-1} data were obtained in the temperature range ~ 291 – 481 K from the high temperature instrument due to strong dissipation, or below ~ 97 K from the low temperature instrument. Values were nevertheless obtained in the temperature interval ~ 97 – 307 K from the low temperature instrument because

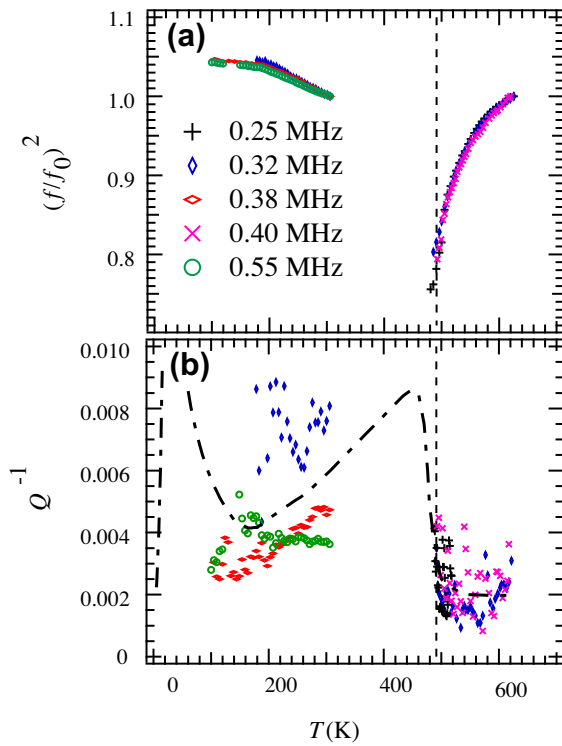


Fig. 2. Temperature dependencies of normalised square of frequency $(f/f_0)^2$ and inverse quality factor Q^{-1} of CaCl_2 determined by RUS. The dashed line is the transition temperature 491 K. The dash-dotted curve shows the pattern of loss behaviour typical of that due to ferroelastic twin wall mobility below the transition point followed by pinning at some lower temperatures.

of the enhanced intensity of spectra, in comparison with those obtained from the high temperature instrument.

Qualitative variations visible in the raw spectra (Fig. 1) are entirely consistent with predictions of softening of the shear modulus as the expected tetragonal \leftrightarrow orthorhombic transition temperature of 491 K (Bärnighausen et al., 1984; Anselment, 1985; Unruh et al., 1992; Unruh, 1993) is approached from either side. The total softening between 626 and 481 K is $\sim 25\%$. Also as anticipated, values of Q^{-1} are small (low attenuation) in the stability field of the tetragonal phase but increase abruptly in the stability field of the orthorhombic phase, to the extent that resonance peaks could no longer be detected between 481 K and room temperature in spectra from the high temperature instrument.

The temperature dependencies of E' , E'' and $\tan\delta$ obtained by DMA at frequencies of 0.1–50 Hz are shown in Fig. 3. Results for $(f/f_0)^2$ and Q^{-1} obtained by RUS at ~ 0.3 MHz are also included for comparison. Note that the DMA data extend through the temperature interval between room temperature and 481 K where no resonance peaks were observed in the RUS spectra. E' increases smoothly with falling temperature from 771 to 651 K, essentially as would be expected for a material with normal thermal expansion, but then softening begins below ~ 550 K. There is a distinct, though rounded minimum at ~ 470 K which is not obviously dependent on frequency. A smooth increase (stiffening) then occurs down to 378 K. This pattern of softening and stiffening occurs in a temperature interval which is in the vicinity of the expected phase transition. In marked contrast with the RUS results, however, there is no evidence for any acoustic loss as $\tan\delta$ remains at a relatively low value for all frequencies at all temperatures below 650 K.

Above ~ 650 K, there are significant increases in $\tan\delta$ which vary systematically with frequency such that the steepest increase is

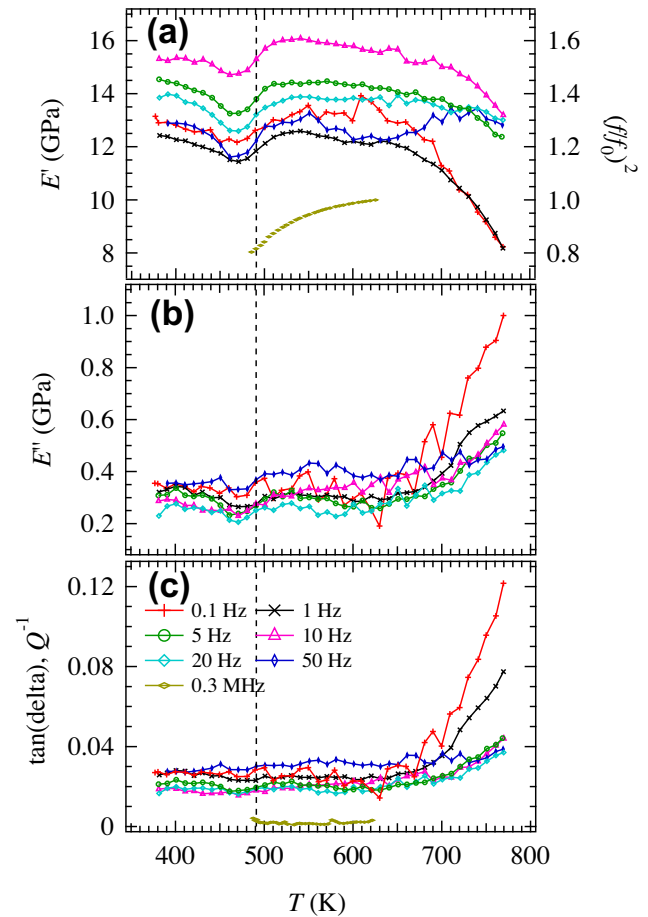


Fig. 3. Temperature dependencies of storage modulus E' , loss modulus E'' and dissipation $\tan\delta$ measured at different frequencies (0.1–50 Hz) by DMA for CaCl_2 during cooling with the cooling rate of 3 K/min. The normalised square of frequency $(f/f_0)^2$ and inverse of quality factor Q^{-1} determined by RUS at high frequencies ~ 0.3 MHz are also shown for comparison. The dashed line is the transition temperature 491 K. Increases in $\tan\delta$ at high temperatures are most likely due to the influence of grain boundaries.

seen at 0.1 Hz and the smallest increase at 50 Hz. These changes in $\tan\delta$ at high temperatures also correlate, more or less, with changes in E' , which shows marked softening at 0.1 Hz and nearly constant values at 50 Hz. A strong anelastic effect is implied and is likely to be due to the influence of grain boundaries as the melting point (1045 K for anhydrous CaCl_2 , Patnaik, 2002) is approached.

4. Discussion

Porosity leads to lower values of elastic moduli than in a fully dense sample (Ren et al., 2009). The high porosity of the samples used here therefore precludes the possibility of obtaining more widely useful data for absolute values of shear or bulk moduli. However, this does not reduce the significance of the data on a relative scale. Measured values of the moduli will depend on a combination of the elastic properties of the grains, with finite stiffness, and of the pores, with zero stiffness. In this sense, a porous sample can be thought of as a two-phase assemblage and, so long as strain is not accommodated entirely by motion along grain boundaries, the frequencies of resonance modes in an RUS experiment will depend predominantly on shear moduli of the crystalline phase. Grain boundary motion leads to distinct anelastic losses which have been extensively characterised by Tan et al. (2001), Jackson

et al. (2002) and Faul and Jackson (2005), for example. The effects become significant at low frequencies and temperatures approaching the melting point. There is evidence of anelastic behaviour of this type at DMA frequencies and temperatures above ~ 650 K (see below). Given that the grain boundary loss mechanism is thermally activated and that grain boundary motion will therefore shift to higher temperatures with increasing frequency of applied stress, it is most unlikely that there will be any measurable contribution to the elastic properties from grain boundary motion in data collected at RUS frequencies and at temperatures in the vicinity of the ferroelastic phase transition of CaCl_2 . Variations of the resonance frequencies and loss parameters can therefore be used as robust measures of the overall elastic and anelastic behaviour.

The $P4_2/mmm \leftrightarrow Pnm$ transition in CaCl_2 displays all the classic features of a pseudoproper ferroelastic phase transition which is second order in character (Unruh et al., 1992; Unruh 1993, 1995; Valgoma et al., 2002). On the basis of lattice parameter data presented in Unruh (1993), the symmetry-breaking shear strain, $(e_1 - e_2)$, exceeds 4% at 0 K, and scales with temperature as $(e_1 - e_2) \propto q^2 \propto (T_c^* - T)$, where q is the order parameter and T_c^* is the transition temperature. In addition, there is a volume strain of over 1% which is made up of a large contraction in the (001) plane, $(e_1 + e_2) \approx -0.01$, and a much smaller contraction along [001], $e_3 \approx -0.001$. The transition is driven by a soft optic mode and the driving order parameter, q , couples bilinearly with the symmetry-breaking strain as $\lambda(e_1 - e_2)q$, where λ is a strain/order parameter coupling coefficient (Unruh et al., 1992; Unruh, 1993). Based on Raman spectroscopic data for the soft mode and lattice parameter data to follow the strains, the overall pattern of behaviour is consistent with the expectations of Landau theory (Unruh, 1993). A more complete development of the Landau expansion to include predicted variations of the elastic constants has been presented elsewhere for the same transition as a function of pressure in stishovite (Carpenter et al., 2000; Hemley et al. 2000b; Carpenter, 2006).

A quantitative description of the elastic properties of CaCl_2 would need data for the elastic constants of the tetragonal structure which are not yet available. Nevertheless, there are two particular observations which indicate how the bulk, shear and Young's moduli must vary qualitatively. Firstly, the strength of bilinear strain/order parameter coupling is indicated by the difference between T_c^* and the critical temperature, T_c , according to

$$T_c^* - T_c = \frac{2\lambda^2}{a(C_{11}^0 - C_{12}^0)}, \quad (5)$$

where a is the coefficient of the q^2 term in a normal Landau expansion and C_{11}^0 and C_{12}^0 are elastic constants of the tetragonal phase without influence from the transition. From Unruh et al. (1992) the value of $T_c^* - T_c$ is 247 K, consistent with the large observed shear strain and strong strain/order parameter coupling. This leads to a steep softening of $C_{11} - C_{12}$ as $T \rightarrow T_c^*$ from above and of $\bar{C}_{11} - \bar{C}_{12} = \frac{1}{2}(C_{11} + C_{22} - 2C_{12})$ as $T \rightarrow T_c^*$ from below. The second directly relevant observation is the value of ~ 6.5 for the ratio of slopes of the square of the frequency of soft mode below and above T_c^* (Unruh et al., 1992). This ratio is also given by $2b/b^*$, where b is the coefficient of the fourth order term in the Landau coefficient and b^* its value as renormalised by coupling of the strains $(e_1 + e_2)$ and e_3 with q^2 . Such a large observed ratio implies a large renormalisation of b and this is consistent with the large observed values of $(e_1 + e_2)$ in Unruh (1993). Strong coupling of the order parameter with the non-symmetry breaking strains in this way leads to significant softening of the elastic constants $\bar{C}_{11} + \bar{C}_{12} = \frac{1}{2}(C_{11} + C_{22} + 2C_{12})$, C_{33} and C_{23} of the orthorhombic structure. The overall form of the expected elastic anomalies is given in Fig. 9 of Carpenter and Salje (1998) and reproduced here in Fig. 4. The bulk modulus will display the same pattern of

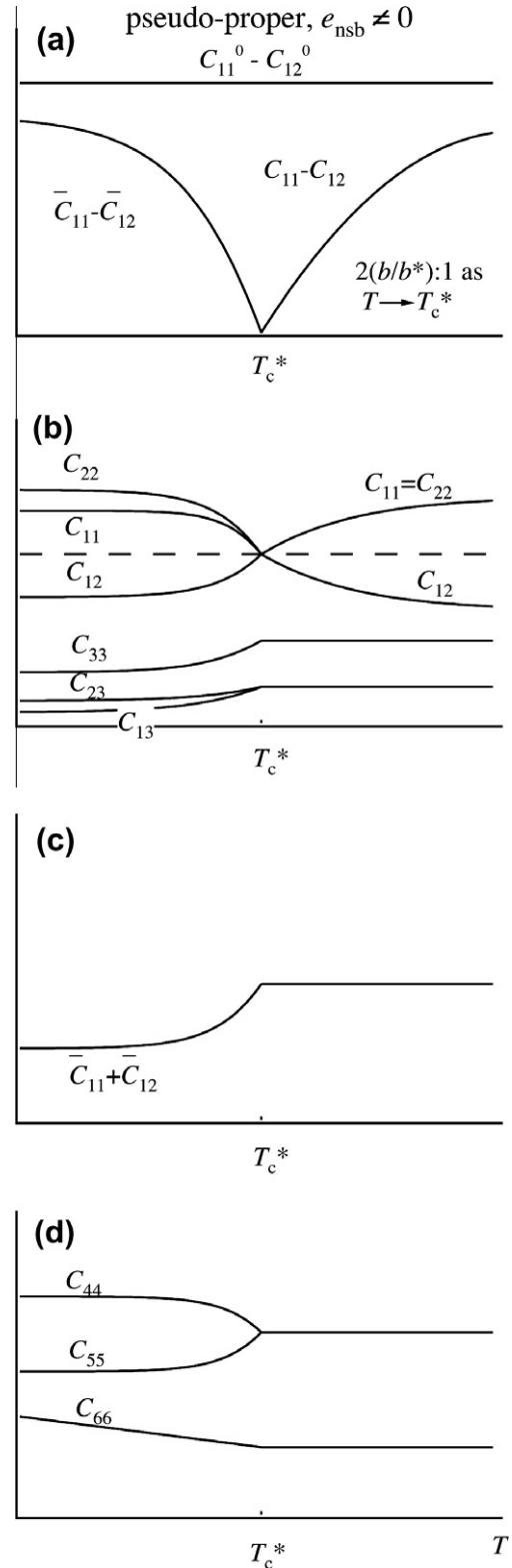


Fig. 4. Schematic form of elastic constant variations expected for a pseudoproper ferroelastic tetragonal \leftrightarrow orthorhombic phase transition. From Fig. 9 of Carpenter and Salje (1998)

evolution as shown for $\bar{C}_{11} + \bar{C}_{12}$, and the shear modulus will have a form which is a combination of $\bar{C}_{11} - \bar{C}_{12}$, C_{44} , C_{55} and C_{66} . The Young's modulus depends on both the shear modulus and the bulk modulus in the usual way, $E = 9KG/(3K + G)$. On this basis, and since both G and E contain contributions from $C_{11} - C_{12}$, the steep

softening shown by $(f/f_0)^2$ as $T \rightarrow T_c^*$ observed by RUS (Fig. 2) and the dip in E' through T_c^* observed by DMA (Fig. 3) are consistent with the model for a pseudoproper ferroelastic transition in CaCl_2 and with the pattern of elastic softening predicted for stishovite (Carpenter et al., 2000). Not included in the Landau description is the influence of fluctuations, which would give some additional softening as the transition is approached from above, particularly of the bulk modulus (cf. Carpenter and Salje, 1998).

The primary objective of this study was to investigate the possibility of anelastic losses accompanying the ferroelastic transition in CaCl_2 as analogue behaviour for the extent to which SiO_2 with the stishovite structure might give rise to seismic attenuation in the Earth's mantle. At DMA frequencies, there is no evidence for any acoustic loss related to the transition and the question then arises as to whether this is due to the experimental conditions representing $\omega\tau \gg 1$ or $\omega\tau \ll 1$. Here ω represents the angular frequency of the applied dynamical stress ($=2\pi f$ for f in Hertz) and τ the relaxation time of the twin walls; maximum dissipation occurs at $\omega\tau = 1$ according to the Debye equation (Nowick and Berry, 1972). At RUS frequencies, the loss behaviour appears to be typical of the influence of ferroelastic twins, implying that the relaxation times for twin walls to respond to an external stress are in the vicinity of $\sim 10^{-6}$ s, and hence, that DMA measurements represent the behaviour at $\omega\tau \ll 1$. Conventional transformation twins have been observed in single crystals of CaBr_2 (Unruh, 1993) and, from the optical observations described above, it appears that twins were present in the polycrystalline sample used here.

Within the stability field of the tetragonal phase, Q^{-1} remains low in spite of the real issue of dealing with a difficult material to prepare and handle. It tends to increase when the transition temperature of 491 K (given by Bärnighausen et al., 1984; Anselment, 1985; Unruh et al., 1992; Unruh, 1993) is approached from above. Immediately below the transition temperature, the dissipation becomes sufficiently large that resonance peaks are not observed. This is characteristic of twin wall mediated superattenuation, as observed in LaAlO_3 (Carpenter et al., 2010). In the interval where there are no data for Q^{-1} due to the strong attenuation, a plateau of attenuation would be expected, by analogy with the dissipation behaviour of both acoustic and dielectric properties at ferroelectric transitions, which is attributed to viscous movement of twin walls. The viscous drag may be understood in terms to the disruption of phonons behind the moving walls (Combs and Yip, 1983; Huang et al., 1992; Wang et al., 1996; Harrison et al., 2004a). At lower temperatures, the improved resolution of the low temperature RUS head reveals the presence of broad RUS peaks with a tendency for Q^{-1} to reduce with falling temperature, corresponding to the lower temperature part of the expected plateau region. Below ~ 100 K the peaks seem again to disappear, though some relatively sharp resonances may be present in the rather noisy spectra collected at the lowest temperatures. A peak of dissipation in this temperature range would be due to freezing of the twin wall motion if it follows the characteristic behaviour of other systems. Hence, although the data for Q^{-1} are incomplete, the present observations are at least consistent with the pattern of loss behaviour reported for LaAlO_3 by Harrison et al. (2004c) (and see Fig. 6 of Carpenter et al., 2010). This pattern is shown by the dash-dotted curve in Fig. 2b.

From these observations, it appears that CaCl_2 behaves in exactly the manner expected for other ferroelastic materials with respect to strain evolution, elastic softening and acoustic losses. There is no reason to suppose that the softening and dynamic loss mechanisms would be different for essentially the same transition in stishovite and the only remaining questions, in terms of analogue properties, are the relative magnitudes of strain/order parameter coupling for the softening, and the relative relaxation times of twin wall motion for the dissipation. The magnitudes of strain coupling effects are already reasonably well constrained

for stishovite (Carpenter et al., 2000; Hemley et al., 2000b) while relaxation times will need to be determined experimentally. If the relaxation behaviour is more or less the same between the two systems, it follows that the velocities of seismic waves through a rock containing twinned, orthorhombic stishovite should be determined by the relaxed elastic constants, i.e. including substantial motion of the twin walls. Comparison with experimental results from single crystals of LaAlO_3 perovskite at low frequencies in its superelastic regime (Harrison and Redfern, 2002; Harrison et al., 2004b) suggests that the effective value of $\bar{C}_{11} - \bar{C}_{12}$ could be as low as $\sim 10\%$ of the intrinsic value, which excludes the influence of the twin walls. In a polycrystalline sample, i.e. a rock, the total magnitude of the twin wall related softening will be less than this, because only some proportion of the grains will have twin walls orientated in such a way that they experience the maximum displacement in response to a given orientation of shear stress (Harrison et al., 2003). Even so, the effective softening should still be greater than the intrinsic softening arising from strain/order parameter coupling and the effective shear modulus will be similarly reduced. Harrison et al. (2003) also pointed out that even a small degree of preferred orientation for twinned ferroelastic crystals could lead to enhanced seismic anisotropy because of the sensitivity of twin wall motion to the orientation of an applied shear stress. The likely population of twin orientations in a sheared polycrystalline sample remains to be characterised and Jackson (2007) has argued that operation of a tectonic stress over a geological timescale would result in most grains consisting of a single twin. In tetragonal and rhombohedral perovskites, pairs of ferroelastic twin walls can occur in three or four degenerate orientations, respectively, making this unlikely. In orthorhombic CaCl_2 or stishovite, however, there is only one orientation for the pairs of ferroelastic twin walls at 90° to each other, and a greater possibility exists for long term deformation reducing rather than enhancing the number of twin walls present.

In conclusion from the present considerations of CaCl_2 , the geophysical signal for the presence of orthorhombic stishovite in the mantle should be lowering of acoustic velocities but without significant attenuation. Only if the relaxation times are substantially slower in stishovite, due to the differences in bonding (particularly for rotations of adjacent octahedral against each other in the (001) plane) or to pinning of the twin walls by impurities such as H or Al, would the softening be accompanied by an increase in attenuation. There is still some uncertainty over the location of the phase transition in pressure and temperature space (Ono et al., 2002a; Tsuchiya et al., 2004; Nomura et al., 2010) and of the effect of Al or H impurities (Lakshtanov et al., 2007a, b). It is therefore not yet clear exactly where stishovite in subducted oceanic crust would transform to the orthorhombic structure, but there are now at least clear patterns of predicted elastic and anelastic behaviour for comparison with geophysical observations.

Acknowledgements

Paul A. Taylor, Richard I. Thomson, Ming Zhang, Armin Fuith and Marius Reinecker kindly provided help with experiments. The RUS facilities in Cambridge were established through a grant from the Natural Environment Research Council (grant no. NE/B505738/1) and the present work was funded through grant no. NE/F017081/1. Support for the DMA facilities in Vienna was provided by the Austrian FWF (grant no. P23982-N20).

References

- Akins, J.A., Ahrens, T.J., 2002. Dynamic compression of SiO_2 : a new interpretation. *Geophys. Res. Lett.* 29, 1394.

- Andraut, D., Angel, R.J., Mosenfelder, J.L., Le Bihan, T., 2003. Equation of state of stishovite to lower mantle pressure. *Am. Mineral.* 88, 301–307.
- Andraut, D., Fiquet, G., Guyot, F., Hanfland, M., 1998. Pressure-induced Landau-type transition in stishovite. *Science* 282, 720–724.
- Anselment, B., 1985. The dynamics of the phase transition of rutile in the CaCl_2 type for the example of CaBr_2 and for the polymorphism of CaCl_2 . University of Karlsruhe, Thesis.
- Bärnighausen, H., Bossert, W., Anselment, B., 1984. A second-order phase transition of calcium bromide and its geometrical interpretation, *Acta Crystallogr. A* 40, C96.
- Bolfan-Casanova, N., Andraut, D., Amiguet, E., Guignot, N., 2009. Equation of state and post-stishovite transformation of Al-bearing silica up to 100 GPa and 3000 K. *Phys. Earth Planet. Inter.* 174, 70–77.
- Brodholt, J.P., Helffrich, G., Trampert, J., 2007. Chemical versus thermal heterogeneity in the lower mantle: The most likely role of anelasticity, *Earth Planet. Sci. Lett.* 262, 429–437.
- Carpenter, M.A., 2006. Elastic properties of minerals and the influence of phase transitions. *Am. Mineral.* 91, 229–246.
- Carpenter, M.A., Buckley, A., Taylor, P.A., Darling, T.W., 2010. Elastic relaxations associate with the $Pm\bar{3}m$ - $R\bar{3}c$ transition in LaAlO_3 : III. Superattenuation of acoustic resonances, *J. Phys.: Condens. Matter* 22, 035405.
- Carpenter, M.A., Hemley, R.J., Mao, H., 2000. High-pressure elasticity of stishovite and the $P4_2/mnm \leftrightarrow Pnmn$ phase transition. *J. Geophys. Res.* 105, 10807–10816.
- Carpenter, M.A., Salje, E.K.H., 1998. Elastic anomalies in minerals due to structural phase transitions. *Eur. J. Mineral.* 10, 693–812.
- Carpenter, M.A., Salje, E.K.H., Braeme-Barber, A., Wruck, B., Dove, M.T., Knight, K.S., 1998. Calibration of excess thermodynamic properties and elastic constant variations associated with the $\alpha \leftrightarrow \beta$ phase transition in quartz. *Am. Mineral.* 83, 2–22.
- Carpenter, M.A., Zhang, Z., 2011. Anelasticity maps for acoustic dissipation associated with phase transitions in minerals. *Geophys. J. Int.* 186, 279–295.
- Cohen, R.E., 1992. First-principles predictions of elastic and phase transitions in high pressure SiO_2 and geophysical implications. In: Syono, Y., Manghni, M.H. (Eds.), *High-Pressure Research: Application to Earth and Planetary Science*. American Geophysical Union, Washington, D.C., pp. 425–431.
- Cohen, R.E., 1994. First-principles theory of crystalline SiO_2 . In: Heaney, P.J., Prewitt, C.T., Gibbs, G.V. (Eds.), *Reviews in Mineralogy, 29, Silica: Physical Behavior, Geochemistry, and Materials Applications*. Mineralogical Society of America, Washington, D.C., pp. 369–402.
- Combs, J.A., Yip, S., 1983. Single-kink dynamics in a one-dimensional atomic chain: a nonlinear atomistic theory and numerical simulation. *Phys. Rev. B* 28, 6873–6885.
- Cordier, P., Mainprice, D., Mosenfelder, J.L., 2004. Mechanical instability near the stishovite- CaCl_2 phase transition: Implication for crystal preferred orientations and seismic properties. *Eur. J. Mineral.* 16, 387–399.
- Daraktchiev, M., Harrison, R.J., Mountstevens, E.H., Redfern, S.A.T., 2006. Effect of transformation twins on the anelastic behavior of polycrystalline $\text{Ca}_{1-x}\text{Sr}_x\text{TiO}_3$ and $\text{Sr}_x\text{Ba}_{1-x}\text{SnO}_3$ perovskite in relation to the seismic properties of Earth's mantle perovskite. *Mater. Sci. Eng. A* 442, 199–203.
- Daraktchiev, M., Salje, E.K.H., Lee, W.T., Redfern, S.A.T., 2007. Effect of internal friction on transformation twin dynamics in perovskite $\text{Sr}_x\text{Ba}_{1-x}\text{SnO}_3$ ($x=0.6, 0.8$). *Phys. Rev. B* 75, 134102.
- Driver, K.P., Cohen, R.E., Wu, Z., Miltzer, B., Rios, P.L., Towler, M.D., Needs, R.J., Wilkins, J.W., 2010. Quantum Monte Carlo computations of phase stability, equations of state, and elasticity of high-pressure silica. *Proc. Natl. Acad. Sci. USA* 107, 9519.
- Dubrovinsky, L.S., Belonoshko, A.B., 1996. Pressure-induced phase transition and structural changes under deviatoric stress of stishovite to CaCl_2 -like structure. *Geochim. Cosmochim. Acta* 60, 3657–3663.
- Farla, R.J.M., Jackson, I., Fitz Gerald, J.D., Faul, U.H., Zimmerman, M.E., 2012. Dislocation damping and anisotropic seismic wave attenuation in Earth's upper mantle. *Science* 336, 332–335.
- Faul, U.H., Jackson, I., 2005. The seismological signature of temperature and grain size variations in the upper mantle, *Earth Planet. Sci. Lett.* 234, 119–134.
- Fritz, I.J., 1974. Pressure and temperature dependencies of the elastic properties of rutile (TiO_2). *J. Phys. Chem.* 35, 817–826.
- Gueguen, Y., Darot, M., Mazot, P., Woignard, J., 1989. Q^{-1} of forsterite single crystals. *Phys. Earth Planet. Inter.* 55, 254–258.
- Gung, Y., Romanowicz, B., 2004. Q tomography of the upper mantle using three-component long-period waveforms. *Geophys. J. Int.* 157, 813–830.
- Hahn, C., Unruh, H.G., 1991. Comment on temperature-induced structural phase transition in CaBr_2 studied by Raman spectroscopy. *Phys. Rev. B* 43, 12665–12667.
- Haines, J., Leger, J.M., 1993. Phase transitions in ruthenium dioxide up to 40 GPa: Mechanism for the rutile-to-fluorite phase transformation and a model for the high-pressure behaviour of stishovite SiO_2 . *Phys. Rev. B* 48, 13344–13350.
- Haines, J., Leger, J.M., 1997. X-ray diffraction study of the phase transitions and structural evolution of tin oxides at high pressure: Relationships between structure types and implications for other rutile-type dioxides. *Phys. Rev. B* 55, 11144–11154.
- Haines, J., Leger, J.M., Chateau, C., Bini, R., Ulivi, L., 1998. Ferroelastic phase transition in rutile-type germanium dioxide at high pressure. *Phys. Rev. B* 58, R2909–R2919.
- Haines, J., Leger, J.M., Chateau, C., Pereira, A.S., 2000. Structural evolution of rutile-type and CaCl_2 -type germanium dioxide at high pressure. *Phys. Chem. Miner.* 27, 575–582.
- Haines, J., Leger, J.M., Gorelli, F., Klug, D.D., Tse, J.S., Li, Z.Q., 2001. X-ray diffraction and theoretical studies of the high-pressure structure and phase transition in magnesium fluoride. *Phys. Rev. B* 64, 134110.
- Haines, J., Leger, J.M., Howau, S., 1995. Second-order rutile-type to CaCl_2 -type phase transition in $-\text{MnO}_2$ at high pressure. *J. Phys. Chem. Solids* 56, 965–973.
- Haines, J., Leger, J.M., Schulte, O., 1996. The high-pressure phase transition sequence from rutile-type through to the contunnite-type structure in PbO_2 . *J. Phys.: Condens. Matter* 8, 1631–1646.
- Haines, J., Leger, J.M., Schulte, O., Hull, S., 1997. Neutron diffraction study of the ambient-pressure, rutile-type and the high-pressure, CaCl_2 -type phases of ruthenium dioxide. *Acta Crystallogr. B* 53, 880–884.
- Harrison, R.J., Redfern, S.A.T., 2002. The influence of transformation twins on the seismic-frequency elastic and anelastic properties of perovskite: dynamical mechanical analysis of single crystal LaAlO_3 . *Phys. Earth Planet. Inter.* 134, 253–272.
- Harrison, R.J., Redfern, S.A.T., Bismayer, U., 2004a. Seismic-frequency attenuation at first-order phase transitions: dynamical mechanical analysis of pure and Cd-doped lead orthophosphate. *Mineral. Mag.* 68, 839–852.
- Harrison, R.J., Redfern, S.A.T., Buckley, A., Salje, E.K.H., 2004b. Application of real-time, stroboscopic x-ray diffraction with dynamical mechanical analysis to characterize the motion of ferroelastic domain walls. *J. Appl. Phys.* 95, 1706–1717.
- Harrison, R.J., Redfern, S.A.T., Salje, E.K.H., 2004c. Dynamical excitation and anelastic relaxation of ferroelastic domain walls in LaAlO_3 . *Phys. Rev. B* 69, 144101.
- Harrison, R.J., Redfern, S.A.T., Street, J., 2003. The effect of transformation twins on the seismic-frequency mechanical properties of polycrystalline $\text{Ca}_{1-x}\text{Sr}_x\text{TiO}_3$ perovskite. *Am. Miner.* 88, 574–582.
- Hellwig, H., Goncharov, A.F., Gregoryanz, E., Mao, H.K., Hemley, R.J., 2003. Brillouin and Raman spectroscopy of the ferroelastic rutile-to- CaCl_2 transition in SnO_2 at high pressure. *Phys. Rev. B* 67, 174110.
- Hemley, R.J., Mao, H.K., Gramsch, S.A., 2000a. Pressure-induced transformations in deep mantle and core minerals. *Mineral. Mag.* 64, 157–184.
- Hemley, R.J., Prewitt, C.T., Kingma, K.J., 1994. High-pressure behaviour of silica. In: Heaney, P.J., Prewitt, C.T., Gibbs, G.V. (Eds.), *Reviews in Mineralogy, 29, Silica: Physical Behavior, Geochemistry, and Materials Applications*. Mineralogical Society of America, Washington, DC, pp. 41–81.
- Hemley, R.J., Shu, J., Carpenter, M.A., Hu, J., Mao, H.K., Kingma, K.J., 2000b. Strain/order parameter coupling in the ferroelastic transition in dense SiO_2 . *Solid State Commun.* 114, 527–532.
- Howard, C.J., Kennedy, B.J., Curfs, C., 2005. Temperature-induced structural changes in CaCl_2 , CaBr_2 , and CrCl_2 : a synchrotron X-ray powder diffraction study. *Phys. Rev. B* 72, 214114.
- Huang, Y.N., Wang, Y.N., Shen, H.M., 1992. Internal friction and dielectric loss related to domain walls. *Phys. Rev. B* 46, 3290–3295.
- Jackson, I., 2007. Physical origins of anelasticity and attenuation in rocks. In: Price, G.D. (Ed.), *Mineral Physics, Treatise on Geophysics*, vol. 2. Elsevier, Oxford, pp. 493–525.
- Jackson, I., Fitz Gerald, J.D., Faul, U.H., Tan, B.H., 2002. Grain-size-sensitive seismic wave attenuation in polycrystalline olivine. *J. Geophys. Res.* 107, 2360.
- Jiang, F., Gwanmesia, G.D., Dyuzheva, T.I., Duffy, T.S., 2009. Elasticity of stishovite and acoustic mode softening under high pressure by Brillouin scattering. *Phys. Earth Planet. Inter.* 172, 235–240.
- Kanchana, V., Vaitheeswaran, G., Rajagopalan, M., 2003. High-pressure structural phase transitions in magnesium fluoride studied by electronic structure calculations. *J. Alloys Compd.* 352, 60–65.
- Kaneshima, S., Helffrich, G., 2010. Small scale heterogeneity in the mid-lower mantle beneath the circum-Pacific area. *Phys. Earth Planet. Inter.* 183, 91–103.
- Karato, S.I., Karki, B.B., 2001. Origin of lateral variation of seismic wave velocities and density in the deep mantle. *J. Geophys. Res.* 106, 21771–21783.
- Karki, B.B., Stixrude, L., Crain, J., 1997a. Ab initio elasticity of three high-pressure polymorphs of silica. *Geophys. Res. Lett.* 24, 3269–3272.
- Karki, B.B., Warren, M.C., Stixrude, L., Ackland, G.J., Crain, J., 1997b. Ab initio studies of high-pressure structural transformations in silica. *Phys. Rev. B* 55, 3465–3471.
- Kennedy, B.J., Howard, C.J., 2004. Synchrotron X-ray powder diffraction study of the structural phase transition in CaBr_2 . *Phys. Rev. B* 70, 144102.
- Kingma, K.J., Cohen, R.E., Hemley, R.J., Mao, H.K., 1995. Transformation of stishovite to a denser phase at lower-mantle pressures. *Nature* 374, 243–245.
- Kingma, K.J., Mao, H.K., Hemley, R.J., 1996. Synchrotron X-ray diffraction of SiO_2 to multimegabar pressures. *High Pressure Res.* 14, 363–374.
- Kusaba, K., Kilegawa, T., 2008a. In situ X-ray observation of phase transitions in ZnF_2 under high pressure and high temperature. *Solid State Commun.* 145, 279–282.
- Kusaba, K., Kikegawa, T., 2008b. Stable phase with the $-\text{PbO}_2$ type structure in MgF_2 under high pressure and high temperature. *Solid State Commun.* 148, 440–443.
- Lacks, D.J., Gordon, R.G., 1993. Calculations of pressure-induced phase transitions in silica. *J. Geophys. Res.* 98, 22147–22155.
- Lakes, R.S., 2004. Viscoelastic measurement techniques. *Rev. Sci. Instrum.* 75, 797–810.
- Lakshatnov, D.L., Litasov, K.D., Sinogeikin, S.V., Hellwig, H., Ohtani, E., Bass, J.D., 2007a. Effect of Al^{3+} and H^+ on the elastic properties of stishovite. *Am. Miner.* 92, 1026–1030.
- Lakshatnov, D., Sinogeikin, S.V., Litasov, K.D., Prakupenka, V.B., Hellwig, H., Wang, J., Sanchez-Valle, C., Perrillat, J.P., Chen, B., Somayazulu, M., Li, J., Ohtani, E., Bass, D., 2007b. The post-stishovite phase transition in hydrous alumina-

- bearing SiO₂ in the lower mantle of the earth. *Proc. Natl. Acad. Sci. USA* 104, 13588–13590.
- Lee, C., Gonze, X., 1995. The pressure-induced ferroelastic phase transition of SiO₂ stishovite. *J. Phys.: Condens. Matter* 7, 3693–3698.
- Lee, C., Gonze, X., 1997. SiO₂ stishovite under high pressure: dielectric and dynamical properties and the ferroelastic phase transition. *Phys. Rev. B* 56, 7321–7330.
- Lee, T., Lakes, R.S., Lal, A., 2000. Resonant ultrasound spectroscopy for measurement of mechanical damping: comparison with broadband viscoelastic spectroscopy. *Rev. Sci. Instrum.* 71, 2855–2861.
- Lekic, V., Matas, J., Panning, M., Romanowicz, B., 2009. Measurement and implications of frequency dependence of attenuation. *Earth Planet. Sci. Lett.* 282, 285–293.
- Lodziana, Z., Parlinski, K., Hafner, J., 2001. Ab initio studies of high-pressure transformations in GeO₂. *Phys. Rev. B* 63, 134106.
- Mao, H.K., Shu, J., Hu, J., Hemley, R.J., 1994. Single-crystal X-ray diffraction of stishovite to 65 GPa. *EOS. Trans. Am. Geophys. Union* 75, 662.
- Matas, J., Bukowinski, M.S.T., 2007. On the anelastic contribution to the temperature dependence of lower mantle seismic velocities. *Earth Planet. Sci. Lett.* 259, 51–65.
- Matsui, Y., Tsuneyuki, S., 1992. Molecular dynamics study of rutile–CaCl₂-type phase transitions of SiO₂. In: Syono, Y., Manghani, M.H. (Eds.), *High Pressure Research: Application to Earth and Planetary Sciences*, vol. 67, Terra Scientific Publishing Company, American Geophysical Union, Washington, DC, pp. 433–439.
- McKnight, R.E.A., Carpenter, M.A., Darling, T.W., Buckley, A., Taylor, P.A., 2007. Acoustic dissipation associated with phase transitions in lawsonite, CaAl₂Si₂O₇(OH)₂H₂O. *Am. Miner.* 92, 1665–1672.
- McKnight, R.E.A., Howard, C.J., Carpenter, M.A., 2009. Elastic anomalies associated with transformation sequences in perovskites: I. Strontium zirconate, SrZrO₃. *J. Phys.: Condens. Matter* 21, 015901.
- McKnight, R.E.A., Howard, C.J., Carpenter, M.A., 2009. Elastic anomalies associated with transformation sequences in perovskites: II. The strontium zirconate-titanate Sr(Zr, Ti)O₃ solid solution series. *J. Phys.: Condens. Matter* 21, 015902.
- McKnight, R.E.A., Moxon, T., Buckley, A., Taylor, P.A., Darling, T.W., Carpenter, M.A., 2008. Grain size dependence of elastic anomalies accompanying the α - β phase transition in polycrystalline quartz. *J. Phys.: Condens. Matter* 20, 075229.
- Mechie, J., Sobolev, S.V., Ratschbacher, L., Babeyko, A.Y., Bock, G., Jones, A.G., Nelson, K.D., Solon, K.D., Brown, L.D., Zhao, W., 2004. Precise temperature estimation in the Tibetan crust from seismic detection of the α - β quartz transition. *Geology* 32, 601–604.
- Migliori, A., Maynard, J.D., 2005. Implementation of a modern resonant ultrasound spectroscopy system for the measurement of the elastic moduli of small solid specimens. *Rev. Sci. Instrum.* 76, 121301.
- Nagel, L., O'Keefe, M., 1971. Pressure and stress induced polymorphism of compounds with rutile structure. *Mater. Res. Bull.* 6, 1317–1320.
- Nomura, R., Hirose, K., Sata, N., Ohishi, Y., 2010. Precise determination of post-stishovite phase transition boundary and implications for seismic heterogeneities in the mid-lower mantle. *Phys. Earth Planet. Inter.* 183, 104–109.
- Nowick, A.S., Berry, B.S., 1972. *Anelastic Relaxation in Crystalline Solids*. Academic Press, New York.
- Ono, S., Hirose, K., Murakami, M., Isshiki, M., 2002a. Post-stishovite phase boundary in SiO₂ determined by in situ X-ray observations. *Earth Planet. Sci. Lett.* 197, 187–192.
- Ono, S., Hirose, K., Murakami, M., Isshiki, M., 2002b. Phase boundary between rutile-type and CaCl₂-type germanium dioxide determined by in situ X-ray observations. *Am. Miner.* 87, 99–102.
- Ono, S., Mibe, K., 2011. Determination of the phase boundary of the ferroelastic rutile to CaCl₂ transition in RuO₂ using in situ high-pressure and high-temperature Raman spectroscopy. *Phys. Rev. B* 84, 054114.
- Parlinski, K., Kawazoe, Y., 2000. Ab initio study of phonons in the rutile structure of SnO₂ under pressure. *Eur. Phys. J. B* 13, 679–683.
- Patnaik, P., 2002. *Handbook of Inorganic Chemicals*. McGraw-Hill.
- Perakis, A., Lampakis, D., Boulmetis, Y.C., Raptis, C., 2005. High-pressure Raman study of the ferroelastic rutile–o-CaCl₂ phase transition in ZnF₂. *Phys. Rev. B* 72, 144108.
- Raptis, C., McGreevy, R.L., 1991. Reply to “Comment on ‘Temperature-induced structural phase transition in CaBr₂ studied by Raman spectroscopy’”. *Phys. Rev. B* 43, 12668–12669.
- Raptis, C., McGreevy, R.L., Segulier, D.G., 1989. Temperature-induced structural phase transition in CaBr₂ studied by Raman spectroscopy. *Phys. Rev. B* 39, 7996–7999.
- Ren, F., Case, E.D., Morrison, A., Tafesse, M., Baumann, M.J., 2009. Resonant ultrasound spectroscopy measurement of Young's modulus, shear modulus and Poisson's ratio as a function of porosity for alumina and hydroxygarnet. *Philos. Mag.* 89, 1163–1182.
- Romanowicz, B., 1995. A global tomographic model of shear attenuation in the upper mantle. *J. Geophys. Res.* 100, 12375–12394.
- Salje, E.K.H., 2008. (An)elastic softening from static grain boundaries and possible effects on seismic wave propagation. *Phys. Chem. Miner.* 35, 321–330.
- Shieh, S.R., Duffy, T.S., Li, B., 2002. Strength and elasticity of SiO₂ across the stishovite–CaCl₂-type structural phase boundary. *Phys. Rev. Lett.* 89, 255507.
- Shieh, S.R., Duffy, T.S., Shen, G., 2005. X-ray diffraction study of phase stability in SiO₂ at deep mantle conditions. *Earth Planet. Sci. Lett.* 235, 273–282.
- Tan, B.H., Jackson, I., Fitz Gerald, J.D., 2001. High-temperature viscoelasticity of fine-grained polycrystalline olivine. *Phys. Chem. Miner.* 28, 641–664.
- Thomson, R.I., Rawson, J.M., Howard, C.J., Turczynski, S., Pawlak, D.A., Lukaszewicz, T., Carpenter, M.A., 2010. Ferroelastic phase transitions and anelastic dissipation in the LaAlO₃–PrAlO₃ solid solution series. *Phys. Rev. B* 82, 214111.
- Togo, A., Oba, F., Tanaka, I., 2008. First-principles calculations of the ferroelastic transition between rutile-type and CaCl₂-type SiO₂ at high pressures. *Phys. Rev. B* 78, 134106.
- Tsuchida, Y., Yagi, T., 1989. A new, post-stishovite high-pressure polymorph of silica. *Nature* 340, 217–220.
- Tsuchiya, T., Caracas, R., Tsuchiya, J., 2004. First principles determination of the phase boundary of high-pressure polymorphs of silica. *Geophys. Res. Lett.* 31, L11610.
- Unruh, H.G., 1993. Ferroelastic phase transitions in calcium chloride and calcium bromide. *Phase Transit.* 45, 77.
- Unruh, H.G., 1995. Soft modes at ferroelastic phase transitions. *Phase Transit.* 55, 155–168.
- Unruh, H.G., Mhlenberg, D., Hahn, Ch., 1992. Ferroelastic phase transition in CaCl₂ studied by Raman spectroscopy. *Z. Phys. B: Condens. Matter* 86, 133–138.
- Valgoma, J.A., Perez-Mato, J.M., Garcia, A., Schwarz, K., Blaha, P., 2002. First-principles study of the ferroelastic phase transition in CaCl₂. *Phys. Rev. B* 65, 134104.
- Vinnik, L.P., Oreshin, S.I., Speziale, S., Weber, M., 2010. Mid-mantle layering from SKS receiver functions. *Geophys. Res. Lett.* 37, L24302.
- Walsh, J.N., Taylor, P.A., Buckley, A., Darling, T.W., Schreuer, J., Carpenter, M.A., 2008. Elastic and anelastic anomalies in (Ca, Sr)TiO₃ perovskites: analogue behaviour for silicate perovskites. *Phys. Earth Planet. Inter.* 167, 110–117.
- Wang, H., Liu, X., Li, Y., Liu, Y., Ma, Y., 2011. First-principles study of phase transitions in antiferromagnetic XF₂ (X=Fe, Co and Ni). *Solid State Commun.* 151, 1475–1478.
- Wang, Y.N., Huang, Y.N., Shen, H.M., Zhang, Z.F., 1996. Mechanical and dielectric energy loss related to viscous motion and freezing of domain walls. *J. Phys. IV France* 6, C8-505–C8-514.
- Webb, S., Jackson, I., 2003. Anelasticity and microcreep in polycrystalline MgO at high temperature: an exploratory study. *Phys. Chem. Miner.* 30, 157–166.
- Zhang, L., Wang, Y., Cui, T., Li, Y., Li, Y., He, Z., Ma, Y., Zou, G., 2007. CaCl₂-type high-pressure phase of magnesium hydride predicted by ab initio phonon calculations. *Phys. Rev. B* 75, 144109.
- Zhang, L., Wang, Y., Cui, Ma, Y., Zou, G., 2008. First-principles study of the pressure-induced rutile–CaCl₂ phase transition in MgF₂. *Solid State Commun.* 145, 283–287.
- Zhang, Z., Koppeneiner, J., Schranz, W., Betts, J.B., Migliori, A., Carpenter, M.A., 2010a. Microstructure dynamics in orthorhombic perovskites. *Phys. Rev. B* 82, 014113.
- Zhang, Z., Koppeneiner, J., Schranz, W., Carpenter, M.A., 2010b. Anelastic loss behaviour of mobile microstructures in SrZr_{1-x}Ti_xO₃ perovskites. *J. Phys.: Condens. Matter* 22, 295401.
- Zhang, Z., Koppeneiner, J., Schranz, W., Prabhakaran, D., Carpenter, M.A., 2011. Strain coupling mechanisms and elastic relaxation associated with spin state transitions in LaCoO₃. *J. Phys.: Condens. Matter* 23, 145401.